Region of Attraction in a Power System With Discrete LTCs

Costas D. Vournas, *Fellow, IEEE*, and Nikos G. Sakellaridis, *Student Member, IEEE*

***Abstract*—This paper extends some previously obtained results on load tap changer (LTC) stability and derives detailed conditions for the stability of a dynamical system consisting of discrete LTC transformers based on Lyapunov's direct method and its extension according to LaSalle's Invariance Principle. The exact region of attraction of a two LTC system is constructed based upon tap position and controlled voltage values. Generalizations and extensions are finally discussed in the framework of extracting rules for post-load-shedding stability.**

***Index Terms*—Discrete systems, load shedding, load tap changers (LTCs), Lyapunov methods, power systems.**

I. Introduction

THE QUESTION OF load tap changer (LTC) stability has been investigated since the 1980s [1], [2] in the framework of the early investigations of the phenomena associated with voltage stability and collapse. Even though many important aspects of voltage stability analysis have been since explained and clarified [3], [4] little progress has been made towards a satisfactory theoretical background for LTC stability taking into account their discrete (or even hybrid) nature and applying to a multi-bus power systems. On the contrary, in many instances LTC analysis is performed considering approximate continuous models that neglect the effect of deadbands and the constant rate of changing taps.

On the other hand, the question of determining the appropriate amount of load to be shed during emergency power system conditions has emerged as a key research topic in recent years [5], [6]. One important aspect of this determination is that the amount of load shedding should guarantee not only the existence of a stable post-shedding equilibrium, but also that the trajectory of system response will be attracted to this equilibrium. This condition is time dependent and is usually checked using simulation and a trial and error procedure [7]. Thus, the determination of the region of attraction of a stable equilibrium is a critical problem for defining the suitable amount for load shedding during an emergency.

In this paper, we attempt to open again the discussion on the exact region of attraction of LTC systems, which seems to have been abandoned in the last decade. To do this, we suggest a formulation where the tap ratio variable corresponds (at equilibrium) to the network side voltage of the LTC, thus providing the equilibrium condition in the form of a PV curve. Following this, we propose an extension of the results presented in [2] without the simplifying use of decoupled load flow modeling and relaxing the constraint of purely reactive load, which is overly restrictive.

We also explicitly define the LTC equilibrium condition using voltage deadband, which is an essential characteristic of discrete LTC systems. This formulation generalizes the equilibrium points of continuous systems to equilibrium sets for discrete systems. The LaSalle invariance principle [8], [9] is used to prove the stability and at the same time to provide the exact region of attraction of a stable equilibrium set. As will be seen, this region is larger than that constructed by hyperboxes [2]. The obtained criteria for stability are expressed in terms of distribution side voltage, as well as tap ratios. It should be noted that this paper deals with monotonic behavior of system trajectories. In [10], [11], and [12] conditions for oscillatory behavior and deadband size have been established. In this paper we consider that the above conditions hold and concentrate on discrete systems, in which the only attractors are disjoint equilibrium sets.

The paper is organized as follows. Section II introduces a necessary mathematical background for system stability analysis. In Section III a general LTC dynamic model is presented along with equilibrium conditions in the cases of neglecting and of explicitly including the deadband effect. The exact region of attraction for a two-LTC system is systematically constructed in Section IV and extensions of the results are discussed. Finally, Section V summarizes the conclusions of the paper and possible future work to be done.

II. Mathematical Background

Before proceeding to the analysis, some necessary terms and definitions are given below.

- J_+ is the set of nonnegative integers.
- $\Re^m$ is the m-dimensional Euclidean space with $||x||$ the Euclidean norm.
- For $x \in \Re^m$ and $H \subset \Re^m$ the distance of x from set H is $d(x,H) = \inf\{||y-x|| : y \in H\}$.
- Consider the mapping $f : \Re^m \to \Re^m$ and the difference equation $x^{k+1} = f(x^k)$. The solution to the initial value problem

$$x^{k+1} = f(x^k), x^0 = x(0) \tag{1}$$

  is $x^k = f^k(x^0)$, where f^k is the kth iteration of $f : f^{k+1} = f(f^k)$ and $f^0 = I$ is the identity mapping. The sequence x^k for $k = 1, 2, \ldots$ is called a trajectory.
- $f^k(H) \to H$ as $k \to \infty$ means $d(f^k(x), H) \to 0$, where $k \in J_+$.

Manuscript received July 12, 2005; revised November 7, 2005. This paper was recommended by Associate Editor A. Hiskens.

The authors are with the National Technical University of Athens, Zografou 15780, Greece (e-mail: vournas@power.ece.ntua.gr; nsakell@central.ntua.gr).

Digital Object Identifier 10.1109/TCSI.2006.875173

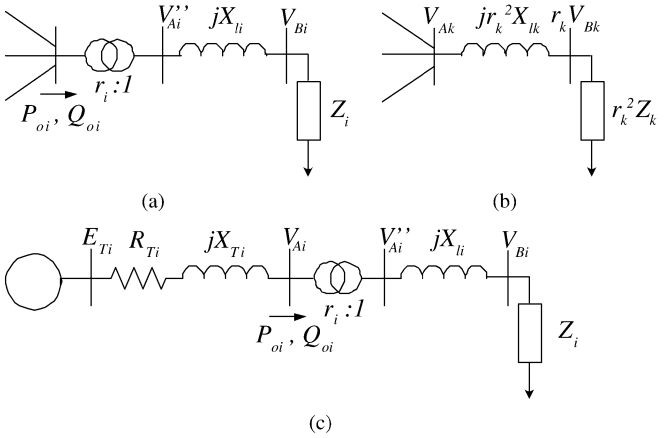

Fig. 1. Power system with m radial LTCs.

- The closure of a set H, denoted by $\bar{H}$, is $\bar{H} = \{x : d(x, H) = 0\}$.
- A set H is said to be stable, if for any neighborhood U of H (an open set containing $\bar{H}$), there is a neighborhood W of H such that $f^k(W) \subset U$ for all $k \in J_+$.
- A set H is said to be an attractor if there is a neighborhood U of $\bar{H}$ such that $x \in U$ implies $f^k(x) \to \bar{H}$ as $k \to \infty$. H is asymptotically stable if it is both stable and an attractor.
- Relative to f a set H is said to be positively (negatively) invariant if $f(H) \subset H (H \subset f(H))$. The set is invariant if $f(H) = H$.
- Let $V : \Re^m \to \Re$. Relative to (1) the derivative of V is defined as follows:

$$\dot{V}(x) = V(f(x)) - V(x). \tag{2}$$

- Let H be any set in $\Re^m$. We say that $V_{\rm LP}$ is a Lyapunov function of (1) on H if (i) $V_{\rm LP}$ is continuous and (ii) $\dot{V}_{\rm LP} \leq 0$ for all $x \in \Re^m$.
- The region of attraction $\mathcal{R}(H)$ of a stable set H is the set of all x such that $f^k(x) \to H$ as $k \to \infty$.

The following is an established theorem from [8] and is related with continuous mappings. Its extension to discontinuous systems, as the one considered in this paper, is given in [9].

Theorem 1: Let H be a bounded open positively invariant set. If (i) $V_{\rm LP}$ is a Lyapunov function of system (1) on H, (ii) $M \subset H$ with M the largest invariant set in H, then M is an attractor and $\bar{H} \subset \mathcal{R}(M)$. If (iii) additionally $V_{\rm LP}$ is constant on M, then M is asymptotically stable.

III. Equilibrium Conditions

Consider a general power system with m loads. All loads are on the secondary (controlled voltage) bus of radial LTC transformers [Fig. 1(a)]. We define $X \subset \Re^m$ the space of permissible LTC ratios $r_i^{\min} \leq r_i \leq r_i^{\max}$ with $i = 1, \ldots, m$. The equilibrium conditions will be examined considering cases with and without deadband. Even though tap ratios take on discretized values, the space X is considered to be compact.

A. Continuous System

For each LTC in a general power system the equilibrium condition is expressed as $V_{Bi} = V_{oi}$, where V_{Bi} is the secondary voltage of the ith LTC and V_{oi} is its reference value. Under this condition, whatever the load dependence on voltage the active and reactive power P_{oi}, Q_{oi} absorbed by the LTC transformer is constant [4]. For impedance loads in particular, P_{oi}, Q_{oi} are given by [see Fig. 1(a)]

$$P_{oi} + jQ_{oi} = \left(\frac{V_{oi}}{|Z_i|}\right)^2 (Z_i + jX_{li}). \tag{3}$$

At this point, we make the following assumptions.

Assumption 1: All loads are linear (constant admittances).

Assumption 2: Generators can be represented by voltage sources (either constant terminal voltage or regulating machines, or constant EMF for rotor limited machines).

Under Assumption 1, with constant taps $r_k, k \neq i$, transformers can be represented as equivalent impedances (Fig. 1(b)). Using both Assumptions 1 and 2, the network seen from the primary of transformer i can be represented by a Thevenin equivalent, as shown in Fig. 1(c).

Thus, for given taps $r_k, k \neq i$, the equilibrium condition for LTC$_i$ reduces to a bi-quadratic equation

$$V_{Ai}^4 - \left[E_{Ti}^2 - 2\left(P_{oi}\, R_{Ti} + Q_{oi}\, X_{Ti}\right)\right] V_{Ai}^2 + \left(P_{oi}^2 + Q_{oi}^2\right)\left(R_{Ti}^2 + X_{Ti}^2\right) = 0. \tag{4}$$

Note that E_{Ti}, R_{Ti}, and X_{Ti} are functions of r_k with $k \neq i$. The positive solutions for V_{Ai} correspond to unique r_i values according to the formula

$$\hat{V}_{Ai} = r_i\, \hat{V}_{oi} \left(1 + j\frac{X_{li}}{Z_i}\right) \tag{5}$$

where $\hat{V}$ is the phasor corresponding to voltage V. With all other taps fixed, (4) for each i defines an $m-1$ manifold in X space which consists of two branches, one of high voltage (high tap) and one of low voltage (low tap) values. The two branches bifurcate at the point where the discriminant of (4) becomes zero. We call the corresponding manifold LTC$_i$ equilibrium manifold, and its two branches high- and low-voltage LTC$_i$ equilibrium branches respectively.

This formulation preserves the quadratic nature of equilibrium conditions used in [2] to derive several important results, whereas it is much more general as it allows the representation of both active and reactive loads. However, this formulation is still approximate, since in real systems the generator active power is fixed by the prime mover, and thus a considerable nonlinearity is introduced. This nonlinearity will not be considered in this paper.

For the case where generators are represented as voltage sources the propositions of [2] concerning the number and stability of equilibria can be proven for the proposed system by following a similar reasoning. Note, however, that in our formulation, it is the higher value of r (high primary or transmission side voltage) that corresponds to stable equilibrium. Thus, a stable equilibrium can exist only on the intersection

of all high-voltage $\mathrm{LTC}_i, i = 1, \ldots, m$ equilibrium branches, whereas all equilibria defined by intersections of LTC_i equilibrium branches, at least one of which is a low-voltage branch, are unstable [2].

B. Discrete System

The LTCs are now modelled as discrete mechanisms, which can operate at discrete time instants $t^{k+1} = t^k + \Delta T_i$, where ΔT_i depends on the device characteristics, and each tap moves by a specified ratio step Δr_i when the corresponding controlled voltage is outside a deadband

$$d_i = V_{Bi}^{\max} - V_{Bi}^{\min}. \tag{6}$$

The tap ratio dynamics are described by the following system of difference equations:

$$\begin{aligned} r_i^{k+1} &= f\left(r_i^k\right) \\ &= \begin{cases} r_i^k + \Delta r_i, & \text{for } V_{Bi} \geq V_{Bi}^{\max} \\ r_i^k, & \text{for } V_{Bi}^{\min} < V_{Bi} < V_{Bi}^{\max} \\ r_i^k - \Delta r_i, & \text{for } V_{Bi} \leq V_{Bi}^{\min} \end{cases} \end{aligned} \tag{7}$$

where $k \in J_+$ and

$$V_{Bi} = g_i(r_1, \ldots, r_m, G_1, \ldots, G_m, B_1, \ldots, B_m). \tag{8}$$

The size of each tap step Δr_i is assumed to be sufficiently small so that oscillatory behavior is avoided [10]–[12]. The voltages V_{Bi} are given in (8) as functions of tap ratios r_i and load conductances G_i and susceptances B_i.

C. Deadband Effect

Consider a single LTC system with a conductance load G (unity power factor considered and leakage reactance neglected). Setting $Z_i = 1/G$ and $V_{oi} = V_B^{\min}$ (respectively $V_{oi} = V_B^{\max}$, where $V_B^{\min}$ and $V_B^{\max}$ are the lower and upper bounds of the LTC deadband) in (3) and substituting in (4) and (5) we can define two curves in the G, r space, which are shown in Fig. 2. Between these curves the secondary voltage satisfies $V^{\min} < V_B < V^{\max}$ and thus the LTC tap remains unchanged. Therefore, the line segments marked as S and U in Fig. 2 satisfy (for a particular value of $G = G_o$) the equilibrium conditions of the LTC and define two *equilibrium sets* corresponding to the stable and unstable equilibria of the continuous system. The two curves forming the boundary of LTC deadband in (3) are similar to the well known PV curves in voltage stability analysis [4]. The PV curves are produced solving (4) in terms of V_{Ai} as a function of active power and projecting the solutions on the P, V_{Ai} plane for constant Q or constant power factor (for Fig. 2 $Q = 0$). The resemblance of the curves of Fig. 2 to the PV curves is then evident, since for LTC equilibrium r is proportional to $V_A (r = V_A/V_o)$ and G is proportional to $P (G = P/V_o^2)$.

It is also well known from the analysis of PV curves, that on the high-voltage branch increasing tap will reduce the secondary voltage V_B. Thus, for the high-voltage equilibrium set S, $V_B^{\min}$ is above $V_B^{\max}$ and consequently the direction of tap movement is along the arrows shown in Fig. 2 and the set S is stable.

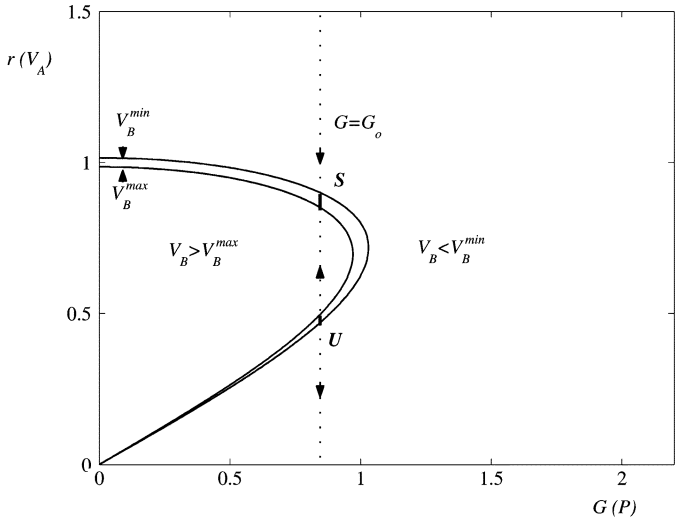

Fig. 2. Equilibria of a single LTC on the $G - r$ space.

The opposite holds for the low-voltage part of the PV curve. Therefore, for the low-voltage equilibrium set U voltage increases with r, i.e., $V_B^{\min}$ is below $V_B^{\max}$. As a result this set is unstable and it forms the boundary of the region of attraction of S, as seen in Fig. 2.

Note that any point on the equilibrium sets satisfies the deadband condition and is thus invariant under (1) and a possible equilibrium point of the discrete system. Of course, the tap r can only assume discrete values (for instance $r = k\,\Delta r$, if the tap step Δr is constant). However, in our analysis we do not concentrate on the actual discrete equilibrium points, but rather on the invariant sets S and U that contain the actual equilibria. Thus, without loss of information we will refer to the invariant sets S and U as equilibrium sets.

These notions are straight forward to generalize in multiple LTC systems. Thus, a set satisfying $V_{Bi}^{\min} < V_{Bi} < V_{Bi}^{\max}$ for all $i = 1, \ldots, m$ is an equilibrium set in state space $X \subset \Re^m$.

It should be noted at this point that in discrete systems even an unstable equilibrium set can be an attractor, because there are trajectories, which actually can be trapped on it. These trajectories correspond to the stable manifold of an unstable equilibrium point in continuous systems.

IV. Region of Attraction

A. Trajectory Directions

In the case of discrete systems, the state space X can be partitioned in regions, on which the direction of trajectories is uniquely determined and it remains constant. The direction depends on Δr_i and ΔT_i, as well as on the relative position of each V_{Bi} in terms of the corresponding deadband. Thus, a direction is a vector with components $0, \pm \Delta r_i / \Delta T_i$ depending on whether V_{Bi} is inside, above, or below the deadband respectively. The direction vector is defined as

$$\mathbf{h} = \left[a_i \frac{\Delta r_i}{\Delta T_i} \right] \tag{9}$$

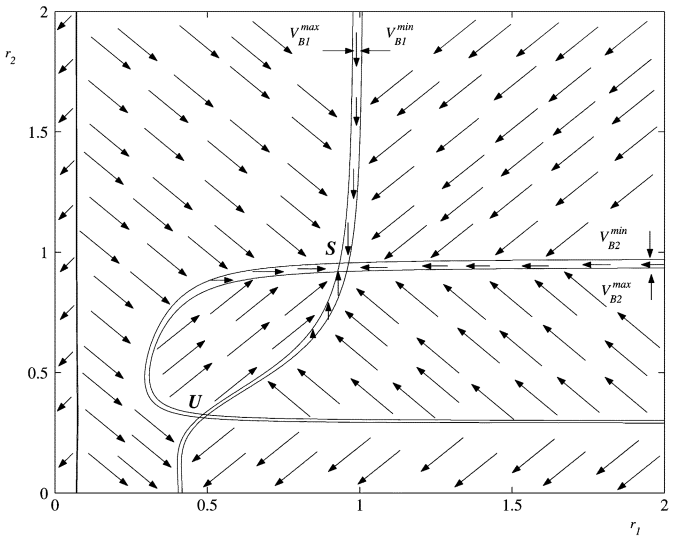

Fig. 3. Direction field on the $r_1 - r_2$ space.

where $a_i = 1$ for $V_{Bi} \geq V_{Bi}^{\max}, a_i = 0$ for $V_{Bi}^{\min} < V_{Bi} < V_{Bi}^{\max}$, and $a_i = -1$ for $V_{Bi} \leq V_{Bi}^{\min}$.

Therefore, outside equilibrium sets (where all $a_i = 0$) there are $3^m - 1$ different trajectory directions in state space. A graphical representation of the 8 directions is depicted in Fig. 3 for the case of two LTCs $(m = 2)$. It should be noted here that the discrete time trajectories actually consist of horizontal and vertical segments in the r_1, r_2 plane corresponding to discrete tap changes. However, effective trajectory movement can be approximated by the directions described by (9).

B. Two-LTC System

We now concentrate on the problem of defining the exact region of attraction of a two-LTC system. The results will provide insight for handling the general case of many LTCs.

The system configuration is shown schematically in Fig. 4, with data given in Table I. P_{1s} and P_{2s} in Table I are the load powers consumed at nominal voltage, for which the region of attraction will be constructed. In the special case of load shedding P_{1s}, P_{2s} correspond to the load demand remaining after the load shedding action. As the generator is represented as a voltage source, Assumptions 1 and 2 of Section III apply. Thus, the continuous LTC system has up to four equilibria and we expect up to four disjoint equilibrium sets when considering deadbands. However, for the numerical data of Table I the system has only two disjoint equilibrium sets. This case is more stressed than that with four equilibria, and thus more representative of system conditions after load shedding.

The active load of each bus is considered independent, while unity power factor is assumed for simplicity. The two loads are fed through lossless transmission lines. The two transformers are ideal (leakage reactances are neglected), with tap ratios r_1 and r_2, respectively.

In the state space portrait of Fig. 3 it is seen that the LTC_i equilibrium manifolds (for a continuous system) correspond now to LTC deadband strips. Similar to the continuous system these strips are separated into high- and low-voltage deadband

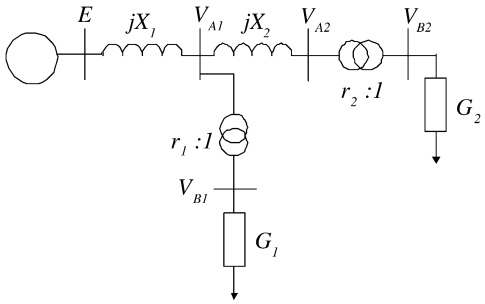

Fig. 4. Two-load system.

TABLE I
TWO-LOAD SYSTEM DATA (P.U)

X_1	X_2	P_{1s}	P_{2s}	E	V_i^{min}	V_i^{max}
0.35	0.25	0.2	0.47	1.0	0.985	1.015

strips. These strips are extracted using (3), (4) and (5) as described in Appendix A.

In this test system, we consider the same time constants for both LTCs, as well as the same tap ratio steps. Therefore, from (9), it follows that the trajectories move along the straight lines: $r_1 + r_2 = c, r_2 - r_1 = c, r_1 = c$ and $r_2 = c$. This property will be exploited in order to construct the stability region of the system.

C. Construction of Region of Attraction

The following analysis of state space X intends in constructing a suitable subset that satisfies the prerequisites of Theorem 1. The equilibrium sets S and U correspond to the intersections of LTC_i deadband strips $(V_{Bi}^{\min} < V_{Bi} < V_{Bi}^{\max})$ and are denoted as

$$S = \left\{\left(r_1^S, r_2^S\right)\right\} \tag{10}$$

$$U = \left\{\left(r_1^U, r_2^U\right)\right\}. \tag{11}$$

In this case, S is the set corresponding to the intersection of high-voltage deadband strips for both LTCs, whereas U is defined by the intersection of the low-voltage deadband strip of LTC_2. In general, S is defined as the high-voltage, high-tap equilibrium set for which

$$r_i^S > r_i^U. \tag{12}$$

The set S is bounded by the following curve segments:

$$S_1^{\min} = \left\{r \in X : V_{B1} = V_{B1}^{\min} \text{ and } d(r, S) = 0\right\} \tag{13}$$

$$S_1^{\max} = \left\{r \in X : V_{B1} = V_{B1}^{\max} \text{ and } d(r, S) = 0\right\} \tag{14}$$

$$S_2^{\min} = \left\{r \in X : V_{B2} = V_{B2}^{\min} \text{ and } d(r, S) = 0\right\} \tag{15}$$

$$S_2^{\max} = \left\{r \in X : V_{B2} = V_{B2}^{\max} \text{ and } d(r, S) = 0\right\}. \tag{16}$$

Segments $U_1^{\min}, U_1^{\max}, U_2^{\min}$ and $U_2^{\max}$ are formed similarly for the equilibrium set U.

Since S corresponds to the high-voltage solution for both LTCs, $S_i^{\max}$ corresponds to lower values of r_i than $S_i^{\min}$. On the other hand, U corresponds to the high-voltage solution of LTC_1

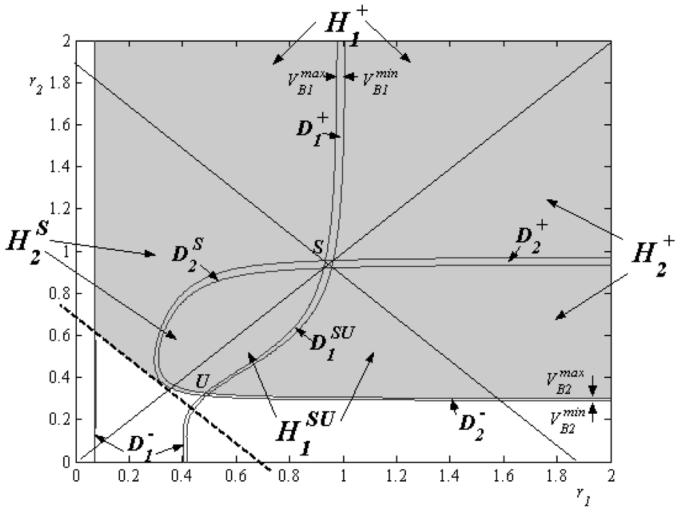

Fig. 5. Geometry of set H.

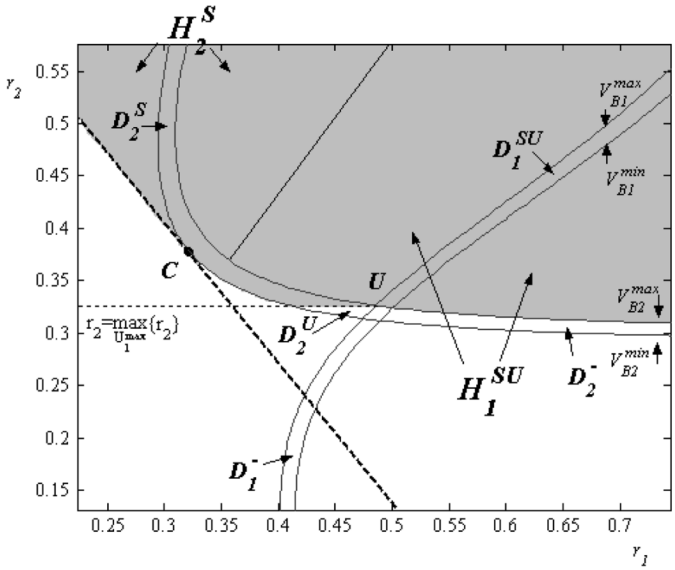

Fig. 6. Detailed region around set U.

deadband, but to the low-voltage solution of LTC_2 deadband. Thus, even though $U_1^{\max}$ corresponds to lower values of r_1 than $U_1^{\min}, U_2^{\max}$ corresponds to higher values of r_2 than $U_2^{\min}$.

We define the deadband strip sets in space X as

$$D_1 = \left\{r \in X : V_{B1}^{\min} < V_{B1} < V_{B1}^{\max}\right\} \tag{17}$$
$$D_2 = \left\{r \in X : V_{B2}^{\min} < V_{B2} < V_{B2}^{\max}\right\}. \tag{18}$$

The direction field shown in Fig. 3 indicates that for a more convenient analysis the previous sets can be decomposed as follows:

$$D_1 = D_1^+ \cup D_1^{SU} \cup D_1^- \cup S \cup U \tag{19}$$
$$D_2 = D_2^+ \cup D_2^{SU} \cup D_2^- \cup S \cup U \tag{20}$$

where D_i^+, D_i^{SU} and $D_i^-, i = 1, 2$, are disjoint sets defined as follows.

- D_i^+ is the connected set where $V_{Bj} \leq V_{Bj}^{\min}$ and which contains $S_j^{\min}$ (but not $U_j^{\min}$), i.e., $S_j^{\min} \subset D_i^+$ and $D_i^+ \cap U_j^{\min} = \emptyset$.
- D_i^{SU} is the connected set where $V_{Bj} \geq V_{Bj}^{\max}$ and which contains both $S_j^{\max}$ and $U_j^{\max}$, i.e., $S_j^{\max} \subset D_i^{SU}$ and $U_j^{\max} \subset D_i^{SU}$.
- D_i^- is the complement of the above sets with respect to D_i with $i, j \in \{1, 2\}$ and $i \neq j$. The above sets are shown in Fig. 5. Note that D_1^- consists of two deadband strips, a high-voltage one below U and a very narrow low-voltage one depicted as an almost vertical line near the r_2 axis in Fig. 5.

Note that the properties of the equilibrium set boundaries discussed above, determine the orientation of the above defined sets with respect to equilibrium sets. Thus, the set D_2^{SU} contains $U_1^{\max}$, which is to the left (lower values of r_1). Since, in this set r_2 is unchanged and V_{B1} is above its deadband, trajectory direction is to the right (increasing r_1). It is thus possible for a trajectory to converge on U. For this reason D_2^{SU} is further partitioned as follows:

$$D_2^{SU} = D_2^S \cup D_2^U \tag{21}$$

where D_2^S and D_2^U are disjoint sets defined as follows:

- D_2^S is the set for which $r_2 > \max_{U_1^{\max}}\{r_2\}$.
- D_2^U is the complement of D_2^S.

The partition of D_2^{SU} is shown in Fig. 6. On the contrary, set D_1^{SU}, which contains $U_2^{\max}$, as seen in Fig. 5 needs no further partition since all trajectories in it move towards increasing r_2 thus leaving behind set U.

We now define the following sets that will allow us to construct the set H for the application of Theorem 1

$$H_1^+ = \{r \in X : f^k(r) \in D_1^+, \text{ for some } k \in J_+\} \tag{22}$$
$$H_2^+ = \{r \in X : f^k(r) \in D_2^+, \text{ for some } k \in J_+\}. \tag{23}$$

Clearly $D_i^+ \subset H_i^+$. Similarly the sets H_1^{SU} and H_2^S contain the corresponding deadband sets and are defined as

$$H_1^{SU} = \left\{r \in X : f^k(r) \in D_1^{SU}, \text{ for some } k \in J_+\right\} \tag{24}$$
$$H_2^S = \left\{r \in X : f^k(r) \in D_2^S, \text{ for some } k \in J_+\right\}. \tag{25}$$

Finally the set H^S contains the equilibrium set S and is defined as

$$H^S = \{r \in X : f^k(r) \in S, \text{for some } k \in J_+ \text{ and } f^k(r) \notin (D_1 \cup D_2) - S\} \tag{26}$$

with $i = 1, 2$.

The set H is now defined as

$$H = H_1^+ \cup H_2^+ \cup H_1^{SU} \cup H_2^S \cup H^S. \tag{27}$$

According to its definition the set H is open, bounded, positively invariant (since no trajectory initiating inside it diverges) and contains only one attractor S, which is the largest invariant subset of H.

The set H in state space X is shown as the shaded area in Figs. 5 and 6. Each component of H is constructed by extending the corresponding deadband (or equilibrium) set along the direction of converging trajectories in each region of the state space. In particular H^S is the set, from which originating trajectories reach S directly without reaching sets D_1 and D_2 first, i.e., it consists of the four diagonal line segments separating the four other component sets of H, as seen in Fig. 5.

We will now determine the boundaries of H in each of the regions of constant trajectory direction outside the deadband sets. First we consider the region between D_1^+ and D_2^+, where trajectories move along lines where $r_1 - r_2 = c$. Starting from the line converging to S in this region and increasing r_1 all trajectories converge to D_2^+ and thus belong to H_2^+. Similarly, for lower r_1 values the trajectories converge to D_1^+ and thus belong to H_1^+. If, as in Fig. 5, the maximum of $c = r_1 - r_2$ on D_2^+ (and the minimum on D_1^+) are encountered on the boundary of X (hard tap limits), then the whole region between D_1^+ and D_2^+, where both voltages are below their deadbands, belongs to H.

Similarly, in the region between D_2^+, D_1^{SU}, and D_2^-, where $V_{B1} < V_{B1}^{\min}$ and $V_{B2} > V_{B2}^{\max}$ trajectories move along lines $r_1 + r_2 = c$. Again, the maximum of $c = r_1 + r_2$ on D_2^+ is encountered on hard limits. The minimum of $c = r_1 + r_2$ on D_1^{SU} is met on $\bar{U}$, which coincides with the minimum of $c = r_1 + r_2$ of the whole region. Thus, entire region specified here belongs to H. In this area the boundary of the region of attraction is the upper limit of D_2^- ($V_2 = V_2^{\max}$). This is not the case in the region between D_1^+, D_2^S, and D_1^-, where $V_{B1} > V_{B1}^{\max}$ and $V_{B2} < V_{B2}^{\min}$. In this region the minimum of $c = r_1 + r_2$ on D_2^S is not on $\bar{U}$. In this case H_2^S is lower bounded by the line

$$r_1 + r_2 = \min_{D_2^S}\{r_1 + r_2\} = r_1^C + r_2^C \tag{28}$$

where C is the tangent point on the $V_{B2} = V_{B2}^{\min}$ curve (lower bound of D_2, see Fig. 6). Note that in this region there are values $r_1 + r_2 > r_1^C + r_2^C$ with $r_1 > r_1^C$ and $r_2 < r_2^C$ which are excluded from set H.

Here, the boundary of the region of attraction is the part of D_1^- (narrow low-voltage deadband strip near the r_2 axis) where $V_1 = V_1^{\max}$, the line given by (28), the lower boundary of $D_2^S (V_2 = V_2^{\min})$, and $r_2 = \max_{U_1^{\max}}\{r_2\}$. The last three boundaries are shown in detail in Fig. 6.

Now a candidate Lyapunov function of (7) on set H is chosen as

$$V_{\mathrm{LP}}(r_1, r_2) = \min_S \left\{ \left| (r_1 + r_2) - \left(r_1^S + r_2^S\right) \right| : \left(r_1^S, r_2^S\right) \in S \right\} \tag{29}$$

where r_1^S and r_2^S are the coordinates of points belonging to S as in (10). Function V_{LP} is continuous. In order to be a Lyapunov function $\dot{V}_{\mathrm{LP}}$ must be negative semidefinite on H, that is $\dot{V}_{\mathrm{LP}} \leq 0$ or $V_{\mathrm{LP}}(r_1^{k+1}, r_2^{k+1}) \leq V_{\mathrm{LP}}(r_i^k, r_2^k)$. The proof is presented in Appendix B.

Since V_{LP} is a Lyapunov function of (7) on H, all prerequisites of Theorem 1 are satisfied and therefore it is deduced that S is an attractor and $\bar{H} \subset \mathcal{R}(S)$. The region of attraction of S has thus been constructed.

D. Discussion and Possible Extensions

Under Assumptions 1 and 2 of Section III, the equilibrium (or deadband) conditions of LTC_i, with all other r_k (for $k \neq i$) constant, were given in (4) and (5) for a general multi-LTC system. This indicates that the geometry of curves forming the deadband strips D_i cannot be more complicated than the one shown in Figs. 3, 5. For instance, it is clear that there are at most two positive solutions of r_i for each r_k. Of course, negative solutions have no physical meaning and are neglected. Note, however, that when including active power injections of generators (or of nonlinear loads), some geometric properties can change. For instance, a low-voltage deadband strip can be prematurely terminated by encountering a singularity [13].

We will now present a general discussion of the above obtained results by describing the region of attraction set H in terms of easily measured variables such as controlled voltages and tap ratios. The discussion refers to the two-LTC system, but these notions can be extended to multi-LTC systems. In these terms the region of attraction consists of the following.

1) The area where both voltages are either inside or below deadband ($V_{Bi} \leq V_{Bi}^{\max}$) due to high tap values ($r_i > r_i^S$). This includes D_i^+ and the area between them.
   Note that it is not likely to encounter this area after a load shedding action in a power system, because this action is applied to a stressed system, where the tap ratios will be usually close to their lower limits.
2) The area where $V_{Bi} > V_{Bi}^{\max}$ for both LTCs.
   In this area taps are increasing thus reducing the stress on the transmission system.
3) The area where $V_{Bi} > V_{Bi}^{\max}$ and $V_{Bj} < V_{Bj}^{\max}, i \neq j$. Here two cases should be considered:
   a) The area where $r_1 + r_2 > r_1^S + r_2^S$.
      This is the area from which trajectories converge on D_1^+ or D_2^+. The voltage above the deadband is restored first in this case. Because of the properties of the equilibrium manifolds, when the LTC_i encounters its deadband both tap ratios are higher than the values of set S and therefore the conditions of case 1 hold again.
   b) The area where $r_1 + r_2 < r_1^S + r_2^S$.
      In this area the sufficient condition to achieve stability is that the secondary voltage below deadband is restored first, so that the trajectories converge on D_1^{SU} or D_2^S respectively. The restoration takes place at lower tap ratio values than the stable equilibrium set and thus an increasing tap action is required so that the system converges to it. It is thus necessary that the active LTC (the one which has not restored its voltage yet) should measure higher voltage than the reference in order to achieve convergence. This useful property is illustrated with the line $r_1 + r_2 = r_1^C + r_2^C$ in Fig. 6.

Note that the counterpart of the stable manifold of the unstable equilibrium that lies on the region of attraction forms the boundary of this region similarly to continuous systems. In this case this counterpart is made up of the deadband strip D_2^U and part of deadband strip D_2^-, as shown in Fig. 7 with the shaded areas.

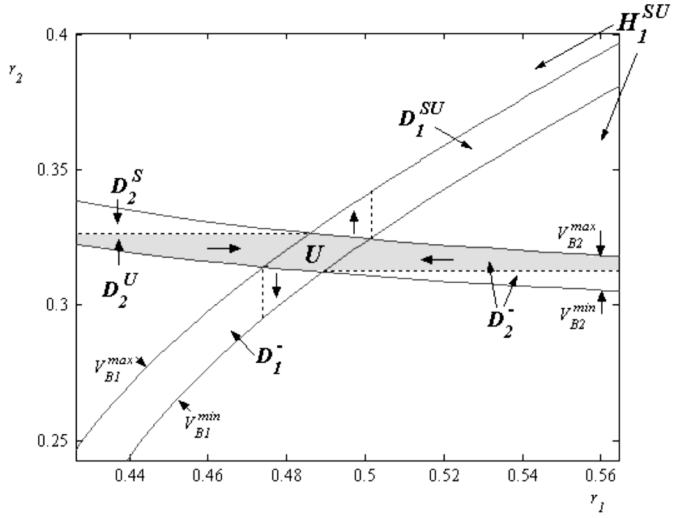

Fig. 7. Counterparts of the stable and unstable manifold of the unstable equilibrium.

Note also that the counterpart of the stable manifold of U belongs in this particular case to the low-voltage deadband strip contributing in the formation of the unstable equilibrium set. When, as in this two-LTC system, the unstable equilibrium set on the boundary of the region of attraction is on the intersection of one low-voltage (LTC_2) and one high-voltage (LTC_1) deadband strip, the following observation can be made concerning the areas where one voltage is above and one below the corresponding LTC deadband (see 3b above):

When the voltage corresponding to LTC_2 (low-voltage strip) is above the deadband and the other voltage below, the region of attraction contains the larger part of the corresponding area (Fig. 5, to the right of D_1^{SU}). On the contrary, in the area where the voltage of LTC_1 (high-voltage strip) is above the deadband and the other voltage below, a relatively smaller part of this area belongs to the region of attraction. This leads to the conjecture that restoration of the voltage corresponding to the LTC, whose low-voltage deadband strip contributes to the unstable equilibrium set (lying on the boundary of the region of attraction) is more valuable than the restoration of the voltage of the LTC corresponding to the high-voltage deadband strip. This can be used to advantage when designing load shedding schemes to avoid voltage collapse. In any case these observations can help in extracting more general results for multi-LTC systems, but this is left for future research.

V. Conclusion

In this paper, the stability of discrete LTC mechanisms in power systems was analyzed in detail. First, equilibrium conditions for continuous LTC systems were derived based on far less restrictive assumptions than in the preexisting literature. Namely the conditions to achieve two smooth solution manifolds for each LTC (a low-voltage and a high-voltage one) are that the generators are represented by voltage sources and the loads are admittances. The equilibrium conditions were subsequently adapted and extended to discrete power systems, where the solution manifolds correspond to deadband strips in state space.

Useful conclusions derived for continuous systems in previous papers were then implemented to the discrete systems. The above deadband strips corresponding to LTC equilibrium conditions, intersect to form equilibrium sets, which are extensions of continuous system equilibrium points. The LaSalle Invariance Principle and its extensions are suitable for the stability analysis of such systems and were used to derive exact conditions for the region of attraction of the stable equilibrium set.

Starting from one- and two-dimensional LTC systems the state space was appropriately decomposed into convenient subsets with specific properties, which can be generalized to higher order systems. A subset of state space forming the counterpart of the stable manifold of an unstable equilibrium in a continuous system was identified for discrete systems. This is simply the set of initial conditions, for which trajectories end up converging on the unstable equilibrium set. It was shown that, similarly to continuous systems, this set forms the boundary of the region of attraction of the stable equilibrium set.

Using the approach followed in this paper, the region of attraction can be defined in terms of easily measured quantities, such as controlled voltages and tap ratios, so that effective rules for a successful load shedding scheme can be drawn. In particular, it was shown that if all controlled voltages are restored above their LTC deadband, attraction towards the stable equilibrium set is achieved. When only some of the controlled voltages are restored, while others remain below the deadband, the attraction to the stable attractor depends upon which secondary voltage will be restored first and the relative tap positions. It was finally discussed that it is more important to restore first the voltage of the LTC, whose low-voltage deadband strip contributes to the unstable equilibrium set that bounds the region of attraction.

Appendix A
Equilibrium Manifolds

Setting $Z_i = 1/G_i$, neglecting leakage reactance X_{li} and regarding lossless transmission lines (3) and (5) become, respectively

$$P_{oi} = V_{oi}^2 G_i, Q_{oi} = 0 \tag{A.1}$$

$$\hat{V}_{Ai} = r_i \hat{V}_{oi} \tag{A.2}$$

where $\hat{V}$ is a phasor. The equilibrium condition of LTC_1 for given tap ratio r_2 then becomes

$$V_{A1}^4 - \left(E_{T1}^2 - 2\,P_{o1}\,R_{T1}\right)\,V_{A1}^2 + P_{o1}^2\,\left(R_{T1}^2 + X_{T1}^2\right) = 0 \tag{A.3}$$

where

$$E_{T1} = \frac{\sqrt{\left[\left(r_2^2/G_2\right)^2 + \left(X_1 + X_2\right)X_2\right]^2 + \left[\left(r_2^2/G_2\right)\,X_1\right]^2}}{\left(r_2^2/G_2\right)^2 + \left(X_1 + X_2\right)^2}\,E \tag{A.4}$$

$$R_{T1} = \frac{\left(r_2^2/G_2\right)\, X_1^2}{\left(r_2^2/G_2\right)^2 + (X_1+X_2)^2} \tag{A.5}$$

$$X_{T1} = \frac{X_1\, \left[\left(r_2^2/G_2\right)^2 + X_1\, X_2 + X_2^2\right]}{\left(r_2^2/G_2\right)^2 + (X_1+X_2)^2}. \tag{A.6}$$

Substituting (A.4), (A.5), (A.6) along with (A.2) for $i = 1$ in (A.3) we have an expression of r_1 as a function of r_2.

Respectively the equilibrium condition of LTC_2 for given tap ratio r_1 is

$$V_{A2}^4 - \left(E_{T2}^2 - 2\, P_{o2}\, R_{T2}\right)\, V_{A2}^2 + P_{o2}^2\, \left(R_{T2}^2 + X_{T2}^2\right) = 0 \tag{A.7}$$

where

$$E_{T2} = \frac{\sqrt{\left(r_1^2/G_1\right)^4 + \left(r_1^2\, X_1/G_1\right)^2}}{\left(r_1^2/G_1\right)^2 + X_1^2}\, E \tag{A.8}$$

$$R_{T2} = \frac{\left(r_1^2/G_1\right)\, X_1^2}{\left(r_1^2/G_1\right)^2 + X_1^2} \tag{A.9}$$

$$X_{T2} = \frac{\left(r_1^2/G_1\right)^2\, (X_1+X_2) + X_1^2\, X_2}{\left(r_1^2/G_1\right)^2 + X_1^2}. \tag{A.10}$$

Again, we substitute (A.8), (A.9), (A.10) along with (A.2) for $i = 2$ in (A.7) so that tap ratio r_2 is expressed in terms of r_1.

Appendix B
Examination of the Sign of $\dot{V}_{\mathrm{LP}}$

Investigating in the subsets of H we have the following.

1 $(r_1, r_2) \in H_1^+$. Three subcases are considered here.

a) $V_{B1} > V_{B1}^{\max}$. In this case r_1 is increasing and r_2 is decreasing. Thus

$$\begin{aligned}\dot{V}_{\mathrm{LP}} &= \left(r_1^{k+1} + r_2^{k+1}\right) - \left(r_1^S + r_2^S\right) - \left(r_1^k + r_2^k\right) \\ &\quad + \left(r_1^S + r_2^S\right) = \left(r_1^k + \Delta r + r_2^k - \Delta r\right) \\ &\quad - \left(r_1^k + r_2^k\right) = 0.\end{aligned} \tag{B.1}$$

b) $V_{B1} < V_{B1}^{\min}$. Here both secondary voltages are below their references, so both ratios are decreasing

$$\begin{aligned}\dot{V}_{\mathrm{LP}} &= \left(r_1^{k+1} + r_2^{k+1}\right) - \left(r_1^S + r_2^S\right) - \left(r_1^k + r_2^k\right) \\ &\quad + \left(r_1^S + r_2^S\right) = \left(r_1^k - \Delta r + r_2^k - \Delta r\right) \\ &\quad - \left(r_1^k + r_2^k\right) = -2\,\Delta r < 0.\end{aligned} \tag{B.2}$$

c) $(r_1, r_2) \in D_1^+$. In this case V_{B1} is in deadband and consequently LTC_1 is inactive, while LTC_2 reduces its ratio so that V_{B2} is increased and reaches its reference. Therefore, $\dot{V}_{\mathrm{LP}}$ is formed as follows:

$$\begin{aligned}\dot{V}_{\mathrm{LP}} &= \left(r_1^{k+1} + r_2^{k+1}\right) - \left(r_1^S + r_2^S\right) - \left(r_1^k + r_2^k\right) \\ &\quad + \left(r_1^S + r_2^S\right) = \left(r_1^k + r_2^k - \Delta r\right) - \left(r_1^k + r_2^k\right) \\ &= -\Delta r < 0.\end{aligned} \tag{B.3}$$

2 $(r_1, r_2) \in H_2^+$. Again three subcases are considered

a) $V_{B2} > V_{B2}^{\max}$. Here V_{B1} is below reference thus r_1 is decreasing, but V_{B2} is increasing

$$\begin{aligned}\dot{V}_{\mathrm{LP}} &= \left(r_1^{k+1} + r_2^{k+1}\right) - \left(r_1^S + r_2^S\right) - \left(r_1^k + r_2^k\right) \\ &\quad + \left(r_1^S + r_2^S\right) = \left(r_1^k - \Delta r + r_2^k + \Delta r\right) \\ &\quad - \left(r_1^k + r_2^k\right) = 0.\end{aligned} \tag{B.4}$$

b) $V_{B2} < V_{B2}^{\min}$. Here both LTCs decrease their ratios in order to increase their secondary voltages

$$\begin{aligned}\dot{V}_{\mathrm{LP}} &= \left(r_1^{k+1} + r_2^{k+1}\right) - \left(r_1^S + r_2^S\right) - \left(r_1^k + r_2^k\right) \\ &\quad + \left(r_1^S + r_2^S\right) = \left(r_1^k - \Delta r + r_2^k - \Delta r\right) \\ &\quad - \left(r_1^k + r_2^k\right) = -2\,\Delta r < 0.\end{aligned} \tag{B.5}$$

c) $(r_1, r_2) \in D_2^+$. Here LTC_2 is inactive and since $V_{B1} < V_{B1}^{\min}\mathrm{LTC}_1$ reduces its ratio to increase secondary voltage. Therefore

$$\begin{aligned}\dot{V}_{\mathrm{LP}} &= \left(r_1^{k+1} + r_2^{k+1}\right) - \left(r_1^S + r_2^S\right) - \left(r_1^k + r_2^k\right) \\ &\quad + \left(r_1^S + r_2^S\right) = \left(r_1^k - \Delta r + r_2^k\right) - \left(r_1^k + r_2^k\right) \\ &= -\Delta r < 0.\end{aligned} \tag{B.6}$$

3 $(r_1, r_2) \in H_1^{SU}$. Following the similar procedure we have

a) $V_{B1} > V_{B1}^{\max}$. Both voltages are above reference, thus:

$$\begin{aligned}\dot{V}_{\mathrm{LP}} &= -\left(r_1^{k+1} + r_2^{k+1}\right) + \left(r_1^S + r_2^S\right) + \left(r_1^k + r_2^k\right) \\ &\quad - \left(r_1^S + r_2^S\right) = -\left(r_1^k + \Delta r + r_2^k + \Delta r\right) \\ &\quad + \left(r_1^k + r_2^k\right) = -2\,\Delta r < 0.\end{aligned} \tag{B.7}$$

b) $V_{B1} < V_{B1}^{\min}$. Tap ratio of LTC_1 is decreasing but tap ratio of LTC_2 is increasing. Consequently, we have

$$\begin{aligned}\dot{V}_{\mathrm{LP}} &= -\left(r_1^{k+1} + r_2^{k+1}\right) + \left(r_1^S + r_2^S\right) + \left(r_1^k + r_2^k\right) \\ &\quad - \left(r_1^S + r_2^S\right) = -\left(r_1^k - \Delta r + r_2^k + \Delta r\right) \\ &\quad + \left(r_1^k + r_2^k\right) = 0.\end{aligned} \tag{B.8}$$

c) $(r_1, r_2) \in D_1^{SU}$. System dynamics in this subset indicates that r_1 remains unchangeable from kth to $k{+}1$th step and r_2 is increasing. Thus, we have

$$\begin{aligned}\dot{V}_{\mathrm{LP}} &= -\left(r_1^{k+1} + r_2^{k+1}\right) + \left(r_1^S + r_2^S\right) + \left(r_1^k + r_2^k\right) \\ &\quad - \left(r_1^S + r_2^S\right) = -\left(r_1^k + r_2^k + \Delta r\right) + \left(r_1^k + r_2^k\right) \\ &= -\Delta r < 0.\end{aligned} \tag{B.9}$$

4 $(r_1, r_2) \in H_2^S$. Three subsets are met by dividing set H_2^S in the same way as before

a) $V_{B2} > V_{B2}^{\max}$. Both voltages are above reference, thus

$$\begin{aligned}\dot{V}_{\mathrm{LP}} &= -\left(r_1^{k+1} + r_2^{k+1}\right) + \left(r_1^S + r_2^S\right) + \left(r_1^k + r_2^k\right) \\ &\quad - \left(r_1^S + r_2^S\right) = -\left(r_1^k + \Delta r + r_2^k + \Delta r\right) \\ &\quad + \left(r_1^k + r_2^k\right) = -2\,\Delta r < 0.\end{aligned} \tag{B.10}$$

b) $V_{B2} < V_{B2}^{\min}$. Here V_{B1} is above reference and r_1 is increasing and V_{B2} is below thus r_2 is decreasing. Therefore, for the sign of $\dot{V}_{\rm LP}$ the following holds:

$$\dot{V}_{\rm LP} = -\left(r_1^{k+1} + r_2^{k+1}\right) + \left(r_1^S + r_2^S\right) + \left(r_1^k + r_2^k\right) - \left(r_1^S + r_2^S\right) = -\left(r_1^k + \Delta r + r_2^k - \Delta r\right) + \left(r_1^k + r_2^k\right) = 0. \quad \text{(B.11)}$$

c) $(r_1, r_2) \in D_2^S$. Inversely to set D_1^{SU} here LTC_2 is inactive but r_1 is increasing and $\dot{V}_{\rm LP}$ becomes

$$\dot{V}_{\rm LP} = -\left(r_1^{k+1} + r_2^{k+1}\right) + \left(r_1^S + r_2^S\right) + \left(r_1^k + r_2^k\right) - \left(r_1^S + r_2^S\right) = -\left(r_1^k + \Delta r + r_2^k\right) + \left(r_1^k + r_2^k\right) = -\Delta r < 0. \quad \text{(B.12)}$$

5 $(r_1, r_2) \in H^S$. The examination of this subset coincides with previous cases and thus it is straightforward that here $\dot{V}_{\rm LP} \leq 0$ as well.

REFERENCES

[1] J. Medanic, M. Ilic-Spong, and J. Christensen, "Discrete models of slow voltage dynamics for under load tap-changing transformer coordination," *IEEE Trans. Power Syst.*, vol. PWRS-2, no. 11, pp. 873–882, Nov. 1987.

[2] C. C. Liu and K. T. Vu, "Analysis of tap-changer dynamics and construction of voltage stability regions," *IEEE Trans. Circuits Syst.*, vol. 36, no. 4, pp. 575–590, Apr. 1989.

[3] C. W. Taylor, *Power System Voltage Stability*, ser. ERPI Power System Engineering Series. New York: McGraw-Hill, 1994.

[4] T. Van Cutsem and C. D. Vournas, *Voltage Stability of Electric Power Systems*. Norwell, MA: Kluwer, 1998.

[5] S. Arnborg, G. Andersson, D. J. Hill, and I. A. Hiskens, "On influence of load modelling for undervoltage shedding studies," *IEEE Trans. Power Syst.*, vol. 13, pp. 395–400, May 1998.

[6] C. Moors, D. Lefebvre, and T. Van Cutsem, "Design of load shedding schemes against voltage instability," in *Proc. IEEE Power Eng. Soc. Winter Meeting*, Singapore, Jan. 2000.

[7] C. Moors, D. Lefebvre, and T. Van Cutsem, "Load shedding controllers against voltage instability: A comparison of designs," in *Proc. IEEE Power Tech.* , Porto, Portugal, Sep. 2001.

[8] J. P. LaSalle, "The stability of dynamical systems," Regional Conference Series in Applied Mathematics Society for Industrial and Applied Mathematics, 1976.

[9] A. N. Michel and K. Wang, *Qualitative Theory of Dynamical Systems*. New York: Marcel Dekker, 1995.

[10] C. D. Vournas and T. Van Cutsem, "Voltage oscillations with cascaded load restoration," in *Proc. IEEE Power Tech.* , Stockholm, Sweden, Jun. 1995.

[11] N. Yorino, M. Danyoshi, and M. Katagawa, "Interaction among multiple controls in tap change under load transformers," *IEEE Trans. Power Syst.*, vol. 12, no. 2, pp. 430–436, Feb. 1997.

[12] Q. Wu, D. Popovic, and D. J. Hill, "Avoiding sustained oscillations in power systems with tap changing transformers," *Int. J. Elect. Power Energy Syst.*, vol. 22, no. 8, pp. 597–605, Aug. 2000.

[13] C. D. Vournas and N. G. Sakellaridis, "Minimum load shedding as a region of attraction problem in hybrid systems," in *Proc. Bulk Power System Dynamics and Control—VI*, Cortina d'Ampezzo, Italy, Aug. 2004.

Costas D. Vournas (S'77–M'87–SM'95–F'05) received the Diploma of Electrical and Mechanical Engineering from the National Technical University of Athens (NTUA), Athens, Greece, in 1975, the M.Sc. degree in electrical engineering from the University of Saskatchewan,Saskatoon, SK, Canada, in 1978, and the Doctor of Engineering degree again from NTUA in 1986.

He is currently Professor in the Electrical Energy Systems Laboratory, School of Electrical and Computer Engineering, NTUA. His research interests include voltage stability and security analysis, as well as power system control.

Nikos G. Sakellaridis was born in 1979. He received the Diploma of Electrical Engineering from the National Technical University of Athens (NTUA), Athens, Greece, in 2003. He is currently working toward the Ph.D. degree in nonlinear power system dynamics in the Electrical Energy Systems Laboratory, School of Electrical and Computer Engineering, NTUA.